

## CHAPTER 5

### INTRODUCTION TO OCEANIC TURBIDITY CURRENTS

#### 5.1 INTRODUCTION

Turbidity currents are the undersea equivalents of sediment-laden river flows. They consist of density-driven bottom currents for which the agent of the density difference is sediment. Turbidity currents occur in the ocean and lakes. They can be sufficiently powerful to erode spectacular submarine canyons. On lower slopes in the deep ocean they are responsible for the deposition of huge submarine fans that are coursed by some of the largest meandering channels in the world.

Turbidity currents, while very similar to subaerial sediment-laden river flows, are different in one fundamental aspect. Even in the absence of sediment river flow continues, because gravity pulls the water down the slope. In the case of turbidity currents in deep water, however, a hydrostatic pressure distribution with the absence of flow is maintained when sediment is not present. Gravity must act on suspended sediment to pull it down the slope; it in turn drags the fluid with it. In the absence of turbulence, however, the sediment must settle out, bringing the flow to a halt. It will be seen that turbidity currents have the capacity to self-accelerate or self-decelerate, a feature that is not seen in river flows.

#### 5.2 GOVERNING EQUATIONS

A turbidity current is schematized in Figure 5.1. A formal derivation of the layer-averaged governing equations can be found in Parker et al. (1986). A brief summary is given here.

The turbidity current is assumed to consist of a dilute suspension of sediment. It is taken to be a sustained event with a head, a long body and the tail. A two-dimensional turbidity current is considered here for simplicity. The streamwise coordinate  $x$  and the upward normal coordinate  $z$  are assumed to be boundary-attached coordinates along the ocean bed. The bed slope  $S$  is assumed to be small. The Boussinesq assumption is invoked for the equations of momentum balance.

The volume concentration of suspended sediment  $\bar{c}$  and streamwise flow velocity  $\bar{u}$ , both averaged over turbulence, are taken to be functions of  $x$ ,  $z$  and  $t$ . Layer thickness  $H$

of the underflow along with layer-averaged concentration  $C$  and streamwise velocity  $U$  are defined as

$$\begin{aligned}UH &= \int_0^\infty \bar{u} dz \\ U^2 H &= \int_0^\infty \bar{u}^2 dz \\ UCH &= \int_0^\infty \bar{u} \bar{c} dz\end{aligned}\tag{5.1a,b,c}$$

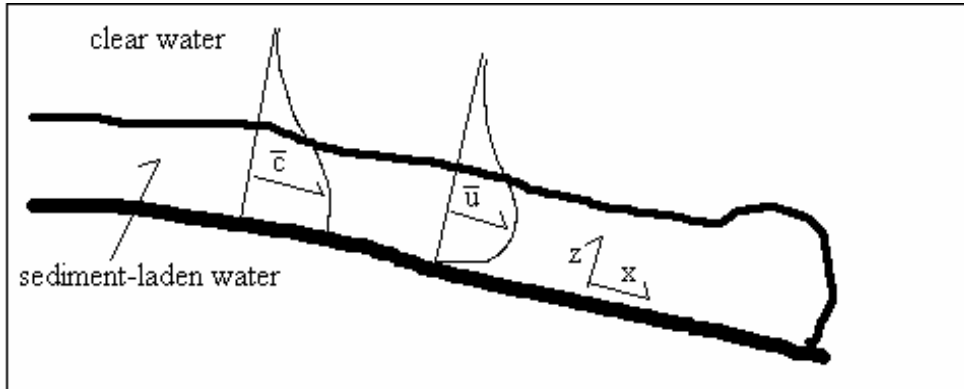


Figure 5.1 Definition diagram for turbidity currents.

Approximate similarity is assumed in the velocity and concentration profiles;

$$\frac{\bar{u}}{U} = f_u(\zeta) \quad \frac{\bar{c}}{C} = f_c(\zeta) \quad \zeta = \frac{z}{H}\tag{3.2}$$

These are further simplified using the crude but useful “top-hat” assumption;

$$f_u(\zeta) = f_c(\zeta) = \begin{cases} 1 & \text{for } 0 \leq \zeta \leq 1 \\ 0 & \text{for } \zeta > 1 \end{cases}\tag{3.3}$$

The governing equations can then be simplified using the boundary layer approximations and integrated to layer-averaged form using the same methods as employed in Chapter 1.

The resulting layer-averaged equations can be written as follows. Water mass balance takes the form

$$\frac{\partial H}{\partial t} + \frac{\partial}{\partial x}(UH) = e_w U\tag{3.4}$$

where  $e_w$  is a dimensionless coefficient of entrainment of ambient water from above. In general it is a function of the bulk Richardson number  $\mathbf{Ri}_b$ , defined as

$$\mathbf{Ri}_b = \frac{RgCH}{U^2} \quad (3.5)$$

The value  $\mathbf{Ri}_b = 0$  yields the highest value of  $e_w$  and corresponds to jet flow; for  $\mathbf{Ri}_b > 1$  the flow becomes subcritical in the Richardson sense and  $e_w$  becomes very small.

Sediment mass balance takes the form

$$\frac{\partial}{\partial t}(CH) + \frac{\partial}{\partial x}(UCH) = v_s(E - r_o C) \quad (3.6)$$

where E is again a dimensionless coefficient of entrainment of bed sediment and

$$r_o = \frac{\bar{c}_b}{C} \quad (3.7)$$

Flow momentum balance takes the form

$$\frac{\partial}{\partial t}(UH) + \frac{\partial}{\partial x}(U^2 H) = -\frac{1}{2} Rg \frac{\partial}{\partial x}(CH^2) + RgCHS - C_f U^2 \quad (3.8)$$

Note that the driving term for the flow,  $RgCHS$  is linearly proportional to concentration, whereas the resistive term contains an approximately quadratic dependence on velocity. Likewise, in the equation of sediment mass balance, the term E, which being dependent on boundary shear stress  $\tau_b$  is in turn dependent on U, adds sediment to the suspension as U increases. The term  $r_o C$  corresponds to increased settling, or loss of sediment from the current as C increases. These terms allow for some fascinating interactions that are best seen in the context of a simpler set of model equations.

The model equations are written as

$$\begin{aligned} \frac{\partial C}{\partial t} &= U^m - C \\ \frac{\partial U}{\partial t} &= C - U^2 \end{aligned} \quad (3.9a,b)$$

The first of these equations models sediment mass balance, with  $U^m$  modeling the entrainment of bed sediment into suspension and  $-C$  modeling the settling of suspended sediment onto the bed. The second of these equations models flow momentum balance,

with  $C$  modeling the downstream pull of gravity on the sediment and  $-U^2$  the resistive force of drag.

The model equations have a fixed point  $(U, C) = (1, 1)$  corresponding to an equilibrium flow similar to the normal state of open channel flow. If  $m > 2$ , however, it is easily shown that this equilibrium is unstable. Unless initial conditions  $(U_i, C_i)$  fall precisely at the fixed point, the flow eventually either accelerates or decelerates away from the fixed point. The process is schematized in Figure 5.2, which shows “igniting” (self-accelerating) and “subsiding” (self-decelerating) fields and a convergence line.

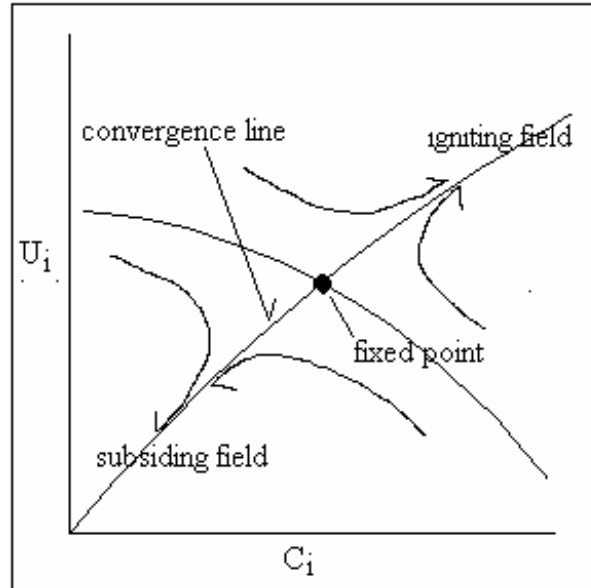


Figure 5.2 Behavior of the model turbidity current.

The essential feature of Figure 5.2 is a galloping instability. If the initial flow velocity and concentration are high enough, the flow can entrain more sediment from the bed, making it heavier. This in turn increases the downstream pull of gravity, accelerating the flow. Acceleration and entrainment can feed into each other leading to ever-swifter flow. On the other hand, if the initial values of  $U$  and  $C$  are too low sediment is lost, the pull of gravity decreases, more sediment is lost etc. as the flow decelerates.

While a full modeling of the above phenomenon using the governing equations of turbidity currents is rather more difficult, the essential result remains unmodified. At high slopes it is found that conditions for ignition are relatively easily obtained. At lower and lower slopes the subsiding zone becomes larger and larger, until a slope is reached at which all turbidity currents die out.

A sample phase diagram calculated from the full model of Fukushima et al. (1985) is shown in Figure 5.3. The simulation is for Scripps Submarine Canyon, a site where self-

accelerative turbidity currents are known to occur with some frequency. The flow is assumed to be steady in time but developing in the downslope direction. The upstream value of current thickness  $H$  is assumed to be 3 m, and  $C_f$  is taken to be 0.004. In the plot  $U$  and  $\Psi = UCH$  denote upstream values. The igniting and subsiding fields are clearly evident in the diagram.

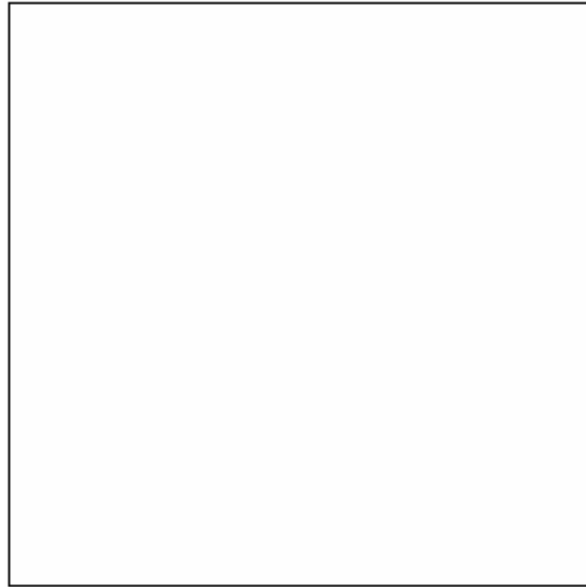


Figure 5.3 Phase diagram computed for Scripps Submarine Canyon

Analyses of the above type can explain the genesis of highly erosive turbidity currents capable of excavating submarine canyons. As slope declines, they can explain the deposition of submarine fans. An extension of the above analysis to two dimensions can explain the maintenance of channels demarcated by high levees even in a purely depositional environment.